Inorg. Chem. **2007**, *46*, 7387−7393

Ethylenebis(triphenylphosphine)platinum as a Probe for Niobium-Mediated Diphosphorus Chemistry

Nicholas A. Piro and Christopher C. Cummins*

Department of Chemistry, Massachusetts Institute of Technology, 77 Massachusetts Avenue, Cambridge, Massachusetts 02139

Received March 16, 2007

Ethylenebis(triphenylphosphine)platinum is used as a trap for the P_2-containing molecule $W(CO)_5(P_2)$, which is eliminated at room temperature from a niobium-complexed diphosphaazide ligand. The rate of $W(CO)_5(P_2)$ elimination is unaffected by the presence of the platinum species. Attempts to generate and trap free P_2 with the platinum ethylene complex were hindered by the direct reaction between the platinum starting material and the P_2 generator, (Mes*NPP)Nb(N[Np]Ar)$_3$. In this case, reductive cleavage of the P–P bond in the diphosphaazide ligand is induced by platinum coordination, resulting in the formation of a trimetallic system with two bridging, three-coordinate phosphorus atoms.

Introduction

The dichotomy that exists between the first-row elements and the higher periods of the main-group elements is striking and well-known.[1] Perhaps it is not better illustrated than by comparing the chemistry of the abundant and notoriously stable dinitrogen molecule with the rare and reactive diphosphorus (P_2) molecule, a species that exists, for the most part, at extreme temperatures (above 1000 K) and low pressures.[1,2] We have recently reported on a transition-metal platform for the generation of P_2, or its synthetic equivalent, under mild conditions.[3] That work demonstrates the use of a niobium terminal phosphide anion for the assembly of a complexed diphosphaazide ligand, P═P═N−Mes* (Mes* = 2,4,6-tri-*tert*-butylphenyl), adding to a small group of heavy azide analogues.[4−6] Thermolysis of the diphosphaazide complex **1** produces the niobium(V) imido (Mes*N)Nb(N[Np]Ar)$_3$ (**2**; Np = neopentyl, Ar = 3,5-dimethylphenyl), with loss of P_2 (Scheme 1). When this reaction is carried out in neat 1,3-cyclohexadiene, the formation of the formal double Diels−Alder adduct of P_2 with two diene equivalents is observed. If instead of being heated the diphosphaazide complex **1** is treated with $W(CO)_5$(THF) (THF = tetrahydrofuran), then complexation takes place and fragmentation producing imido **2** occurs at room temperature (Scheme 1). Under these conditions, the formal trapping of $W(CO)_5(P_2)$ to produce the $W(CO)_5$-complexed double Diels−Alder adduct of P_2 can be accomplished in diethyl ether with merely a stoichiometric quantity of diene present.

The foregoing observations establish these niobium diphosphaazide complexes as remarkable P_2 synthons. We now seek to expand the range of substrates that can act as a trap for the putative P_2 and $W(CO)_5(P_2)$ intermediates.

Metal complexes containing P_n ($n \geq 2$) units have been studied extensively, and the P atoms they contain have come from a variety of sources.[7] The first P_2 complex, $Co_2(CO)_6P_2$, was synthesized in 1973, with the P atoms therein derived from PCl_3.[8] White phosphorus (P_4) has been a particularly common source of P_2 units in transition-metal chemistry.[9−11] Photolytically activated P_4 has been used as well, and P_2 intermediates have been postulated for these reactions,

* To whom correspondence should be addressed. E-mail: ccummins@mit.edu.

(1) Greenwood, N. N.; Earnshaw, A. *Chemistry of the Elements*, 2nd ed.; Butterworth-Heinemann: Oxford, U.K., 1997.
(2) Stevenson, D. P.; Yost, D. M. *J. Chem. Phys.* **1941**, *9*, 403−408.
(3) Piro, N. A.; Figueroa, J. S.; McKellar, J. T.; Cummins, C. C. *Science* **2006**, *313*, 1276−1279.
(4) Brask, J. K.; Fickes, M. G.; Sangtrirutnugul, P.; Durà-Vilà, V.; Odom, A. L.; Cummins, C. C. *Chem. Commun.* **2001**, 1676−1677.
(5) Weber, L. *Angew. Chem., Int. Ed.* **2007**, *46*, 830−832.
(6) Agarwal, P.; Piro, N. A.; Meyer, K.; Müller, P.; Cummins, C. C. *Angew. Chem., Int. Ed.* **2007**, *46*, 3111−3114.
(7) Scherer, O. J. *Acc. Chem. Res.* **1999**, *32*, 751−762.
(8) Vizi-Orosz, A.; Pályi, G.; Markó, L. *J. Organomet. Chem.* **1973**, *60*, C25−C26.
(9) Goh, L. Y.; Chu, C. K.; Wong, R. C. S.; Hambley, T. W. *J. Chem. Soc., Dalton Trans.* **1989**, 1951−1956.
(10) Scherer, O. J.; Ehses, M.; Wolmershäuser, G. *Angew. Chem., Int. Ed.* **1998**, *37*, 507−510.
(11) Figueroa, J. S.; Cummins, C. C. *J. Am. Chem. Soc.* **2003**, *125*, 4020−4021.

10.1021/ic700514u CCC: $37.00
Published on Web 08/03/2007

Scheme 1

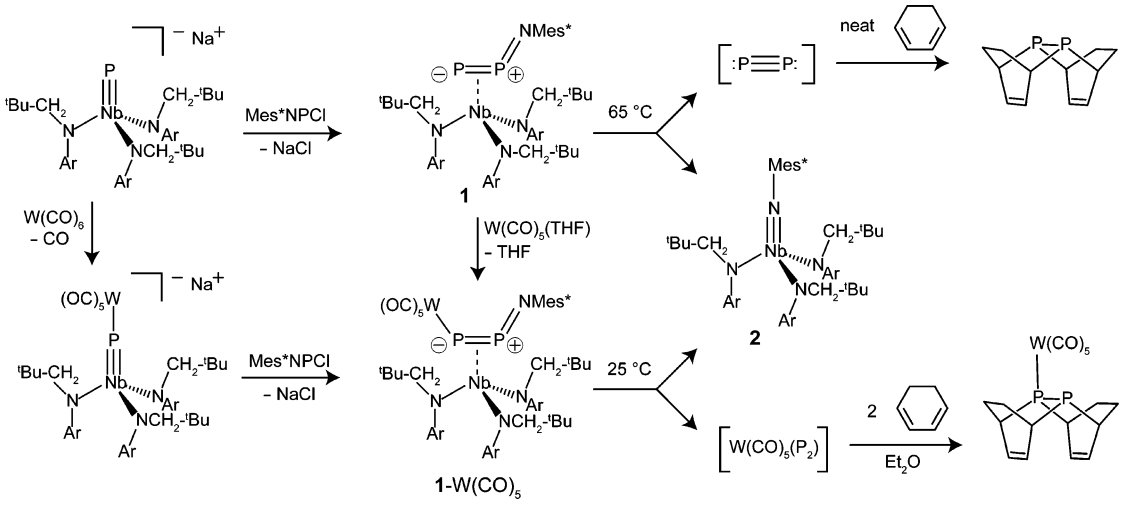

Scheme 2

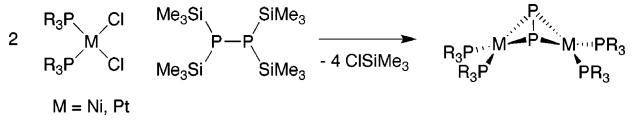

although radical mechanisms can also be invoked.[12−14] P_2 complexes of Ni and Pt that are unsupported by a metal−metal bond have been synthesized from tetrakis(trimethylsilyl)diphosphine (Scheme 2).[15,16] The platinum diphosphorus complex (μ-P_2)[Pt(PPh_3)$_2$]$_2$, in particular, attracted our attention because it seemed likely to be accessible via P_2-trapping chemistry. The labile ethylene ligand in ethylenebis(triphenylphosphine)platinum has made this complex an attractive reagent for facile reactions with element−P π bonds, such as those in diphosphenes[17−19] and phosphaalkynes.[20] It thus seemed an ideal trap for the P_2-containing intermediates generated from diphosphaazide complexes. It is noteworthy that the reaction between this platinum ethylene complex and P_4 has been studied and that it does not generate the P_2 complex.[21] Herein we report our observations on the reactions of niobium diphosphaazide complexes as they ensue in the presence of (C_2H_4)Pt(PPh_3)$_2$.

Experimental Section

General Considerations. All manipulations were performed in a Vacuum Atmospheres model MO-40M glovebox under an atmosphere of purified N_2. Anhydrous-grade, oxygen-free tetrahydrofuran (THF) was purchased from Aldrich and further dried by passing through a column of molecular sieves and stirring with Na for at least 12 h prior to filtration through Celite to remove Na. Hexamethyldisiloxane [$O(SiMe_3)_2$] was vacuum-transferred off sodium benzophenone and stored over molecular sieves. All other solvents were obtained anhydrous and oxygen-free by bubble degassing (N_2) and purification through columns of alumina and Q5.[22] Diethyl ether (Et_2O) was additionally dried by stirring over Na for 12 h, followed by filtration through Celite. Deuterated solvents were purchased from Cambridge Isotope Labs. Benzene-d_6 and toluene-d_8 were degassed and stored over molecular sieves for at least 2 days prior to use. Celite 435 (EM Science), 4 Å molecular sieves (Aldrich), and alumina (EM Science) were dried by heating at 200 °C under a dynamic vacuum for at least 24 h prior to use. The metal complexes (C_2H_4)Pt(PPh_3)$_2$, [(Et_2O)Na][(CO)$_5$WPNb(N[Np]Ar)$_3$], and (Mes*NPP)Nb(N[Np]Ar)$_3$ were prepared according to literature procedures.[3,23] All glassware was oven-dried at temperatures greater than 170 °C prior to use. NMR spectra were obtained on Varian Mercury 300 or Varian Inova 500 instruments equipped with Oxford Instruments superconducting magnets and referenced to residual C_6D_5H (7.16 ppm) or $CHCl_3$ (7.26 ppm). ^{31}P NMR spectra were referenced externally to 85% H_3PO_4 (0 ppm), and ^{195}Pt NMR spectra were referenced externally to K_2PtCl_4 in D_2O (−1624 ppm). Elemental analyses were performed by Midwest Microlab, Indianapolis, IN.

Synthesis of [(Ph_3P)$_2$Pt]$_2$$P_2$W($CO$)$_5$ (3). To a thawing, dark-orange Et_2O solution (4 mL) of [(Et_2O)Na][(CO)$_5$WPNb(N[Np]-Ar)$_3$] (200 mg, 0.18 mmol) was added dropwise a thawing Et_2O solution (2 mL) of Mes*NPCl (58 mg, 0.18 mmol, 1 equiv), affording an immediate color change to dark red. This mixture was allowed to stir for 1 min, and then to it was added a pale-yellow THF solution (6 mL) of (C_2H_4)Pt(PPh_3)$_2$ (275 mg, 0.37 mmol, 2.05 equiv). This mixture was allowed to stir for 135 min while at 22 °C. After this time, the solvent was removed in vacuo and the residue was extracted with 25 mL of a 2:1 toluene/benzene mixture and filtered through Celite to remove NaCl. The yellow filtrate was dried and then suspended in a 1:1 toluene/hexane mixture and stored at −35 °C to precipitate the desired product. This yellow powder was isolated on a sintered glass frit and dried in vacuo to constant mass (198 mg, 0.11 mmol, 60% yield). ^{31}P{^{1}H} NMR (toluene-d_8, 20 °C, 202.5 MHz): δ 27.3 (m, J_{PtP} = 350 Hz), 25.0 (m, J_{PtP} =

(12) Bjarnason, A.; DesEnfants, R. E., II; Barr, M. E.; Dahl, L. F. *Organometallics* **1990**, *9*, 657−661.
(13) Barr, M. E.; Adams, B. R.; Weller, R. R.; Dahl, L. F. *J. Am. Chem. Soc.* **1991**, *113*, 3052−3060.
(14) Chisholm, M. H.; Folting, K.; Scheer, M. *Polyhedron* **1998**, *17*, 2931−2935.
(15) Schäfer, H.; Binder, D.; Fenske, D. *Angew. Chem., Int. Ed. Engl.* **1985**, *24*, 522−524.
(16) Schäfer, H.; Binder, D. *Z. Anorg. Allg. Chem.* **1988**, *560*, 65−79.
(17) Jutzi, P.; Meyer, U.; Opiela, S.; Neumann, B.; Stammler, H.-G. *J. Organomet. Chem.* **1992**, *439*, 279−301.
(18) Phillips, I. G.; Ball, R. G.; Cavell, R. G. *Inorg. Chem.* **1992**, *31*, 1633−1641.
(19) Pietschnig, R.; Niecke, E. *Organometallics* **1996**, *15*, 891−893.
(20) Burckett-St. Laurent, J. C. T. R.; Hitchcock, P. B.; Kroto, H. W.; Nixon, J. F. *J. Chem. Soc., Chem. Commun.* **1981**, 1141−1143.
(21) Scheer, M.; Dargatz, M.; Rufińska, A. *J. Organomet. Chem.* **1992**, *440*, 327−334.
(22) Pangborn, A. B.; Giardello, M. A.; Grubbs, R. H.; Rosen, R. K.; Timmers, F. J. *Organometallics* **1996**, *15*, 1518−1520.
(23) Hartley, F. R. *Organomet. Chem. Rev. A* **1970**, *6*, 119−137.

3510 Hz). ^{1}H NMR ($CDCl_3$, 20 °C, 300 MHz): δ 7.20 (t, J = 9.0 Hz, 12H), 7.06 (t, J = 7.5 Hz, 12H), 6.88 (t, J = 7.5 Hz, 24H). ^{13}C NMR ($CDCl_3$, 20 °C, 75.4 MHz): δ 203.2 (*ax*-CO), 200.1 (*eq*-CO), 135.4 (d, J_{CP} = 43 Hz, *ipso*-Ph), 134.4 (d, J_{CP} = 10 Hz, *o*-Ph), 129.4 (s, *p*-Ph), 127.8 (d, J = 10 Hz, *m*-Ph). ^{195}Pt{^{1}H} NMR (THF, 20 °C, 107.1 MHz): δ −4963 (tt, J_{PPh_3} = 3510 Hz, J_{PP_2} = 350 Hz). IR (C_6D_6, KBr): 2057, 1924, 1885, 1620 cm^{-1}. Elem. anal. Calcd for $C_{77}H_{60}O_5P_6Pt_2W$: C, 50.67; H, 3.31. Found: C, 50.84; H, 3.46.

Synthesis of Mes*NP(PtPPh$_3$)$_2$PNb(N[Np]Ar)$_3$ (4). A red-orange Et_2O solution (7 mL) of (Mes*NPP)Nb(N[Np]Ar)$_3$ (200 mg, 0.20 mmol, 1 equiv) was added at 20 °C to an off-white Et_2O suspension (3 mL) of $(C_2H_4)Pt(PPh_3)_2$ (304 mg, 0.40 mmol, 2.0 equiv). The solution rapidly acquired a deep-maroon hue, and gas evolution was observed. A solid precipitate (PPh_3) was observed in the reaction mixture. The solution was allowed to stir for 20 min, and then it was filtered through a bed of Celite to remove the precipitate. The maroon filtrate was stripped of solvent in vacuo. To the oily residue was added hexane (5 mL), which was then removed in vacuo. The newly formed residue was extracted with hexane (8 mL) and filtered through Celite to remove residual PPh_3. The dark-maroon solution was stored at −35 °C to precipitate the desired product as a brown solid. A small amount of product (20 mg) was isolated by filtration on a frit from this solution. The filtrate was dried, dissolved in toluene, and layered with $(SiMe_3)_2O$. After storage at −35 °C, a larger crop (~100 mg) was isolated by filtration atop a frit. Subsequent crops were isolated from −35 °C solutions of pentane/Et_2O. The combined solids were dried in vacuo to give a dark-maroon-orange powder (220 mg, 0.116 mmol, 58%). The yield is believed to be limited by isolation and not by the conversion. ^{1}H NMR (C_6D_6, 20 °C, 500 MHz): δ 7.93 (m, 12H, *o*-Ph), 7.38 (s, 2H, *m*-Mes*), 7.06 (m, 18H, *m*,*p*-Ph), 6.67 (s, 6H, *o*-Ar), 6.43 (s, 3H, *p*-Ar), 4.75 (s, 6H, NCH_2), 2.14 (s, $ArCH_3$), 1.38 (s, 9H, *p*-Mes*), 1.34 (s, 18H, *o*-Mes*), 0.98 (s, 27H, ^{t}Bu). ^{31}P{^{1}H} NMR (C_6D_6, 20 °C, 121.5 MHz): δ 543 (br pseudo t, Nb*P*), 337 (m, Mes*N*P*), 30.8 (J_{PtC} = 5574 Hz, Pt*P*Ph$_3$). ^{13}C{^{1}H} NMR (C_6D_6, 20 °C, 125.8 MHz): δ 152.2 (*ispo*-Ar), 141.7 (d, J_{CP} = 35 Hz, *ipso*-Mes*), 138.2 (Ar), 137.4 (m, *ipso*-Ph, Mes*), 135.7 (Mes*), 135.3 (Ph), 130.5 (Ph), 129.0 (Ph), 125.2 (Ar), 121.9 (Mes*), 121.6 (Ar), 79.6 (NCH_2), 37.7 ($NCH_2C(CH_3)_3$), 36.8 (*o*-Mes*), 35.2 (*p*-Mes*), 32.3 (Mes*), 31.9 (Mes*), 30.7 ($NCH_2C(CH_3)_3$), 22.2 (ArMe). Elem. anal. Calcd for $C_{93}H_{119}N_4NbP_4Pt_2$: C, 58.79; H, 6.31; N, 2.95. Found: C, 59.28; H, 6.33; N, 2.44.

Kinetics of W(CO)$_5$(P$_2$) Elimination in the Presence of (C$_2$H$_4$)Pt(PPh$_3$)$_2$. A thawing solution (1 mL) of Mes*NPCl (14 mg, 0.045 mmol, 1 equiv) was added to a thawing Et_2O solution (2 mL) of [(Et_2O)Na][(CO)$_5$WPNb(N[Np]Ar)$_3$] (50 mg, 0.045 mmol). This solution was stirred for 30 s before the solvent was removed in vacuo. The residue was extracted with a toluene-d_8 (ca. 1.5 mL) solution of $(C_2H_4)Pt(PPh_3)_2$ (75 mg, 2.2 equiv) and ferrocene (4 mg, used as an internal standard). The resulting mixture was filtered cold through Celite into a sealable (J. Young) NMR tube, which was then frozen for transport to an NMR probe precooled to 10 °C. Four-scan ^{1}H NMR spectra were collected every 372 s for 3 h. The integral of the methylene residue of **1**-W(CO)$_5$ as a function of time, corrected versus the ferrorcene standard, was fit to the first-order rate equation $I(t) = Ae^{-kt} + b$ using the automated routine of *Gnuplot*.[24]

X-ray Diffraction Studies. Diffraction-quality crystals were grown from toluene (**3**), toluene/$(SiMe_3)_2O$ (**4**), THF/Et_2O (**1**-W(CO)$_5$ and [(12-crown-4)$_2$Na][(CO)$_5$WPNb(N[Np]Ar)$_3$]), or Et_2O ([(Et_2O)$_3$Na][(CO)$_5$WPNb(N[Np]Ar)$_3$]) at −35 °C over several days. Crystals were mounted in hydrocarbon oil on a nylon loop or a glass fiber. Low-temperature (100 K) data were collected on a Siemens Platform three-circle diffractometer coupled to a Bruker-AXS Smart Apex CCD detector with graphite-monochromated Mo Kα radiation (λ = 0.710 73 Å) performing ϕ and ω scans. A semiempirical absorption correction was applied to the diffraction data using *SADABS*.[25] All structures were solved by direct or Patterson methods using *SHELXS*[26] and refined against F^2 on all data by full-matrix least squares with *SHELXL-97*.[27] All non-H atoms were refined anisotropically. All H atoms were included in the model at geometrically calculated positions and refined using a riding model. The isotropic displacement parameters of all H atoms were fixed to 1.2 times the U value of the atoms they are linked to (1.5 times for methyl groups). In structures where disorders were present, the disorders were refined within *SHELXL* with the help of rigid bond restraints as well as similarity restraints on the anisotropic displacement parameters for neighboring atoms and on 1,2 and 1,3 distances throughout the disordered components. The relative occupancies of disordered components were refined freely within *SHELXL*. In addition, because of the relatively low-resolution data from the crystal of **4**, rigid bond restraints as well as similarity restraints on anisotropic displacement parameters were applied to the contents of the entire unit cell. Also, fractional occupancies of $(SiMe_3)_2O$ solvent molecules were included in the solution to **4**, which results in fractional atoms in the empirical formula. Further details are available in the Supporting Information (Table S1 and a CIF file) or from the CCDC under deposition numbers 640198−640201.[28]

Computational Studies. All calculations were carried out using ADF 2004.01 from Scientific Computing and Modeling (http://www.scm.com)[29,30] on a four- or an eight-processor Quantum Cube workstation from Parallel Quantum Solutions (http://www.pqs-chem.com).

In all cases, the LDA functional employed was that of Vosko, Wilk, and Nusair (VWN),[31] while the GGA part was handled using the functionals of Becke and Perdew (BP86).[32−34] In addition, all calculations were carried out using the zero-order regular approximation (ZORA) for relativistic effects.[35−37] In all cases, the basis sets were triple-ζ with two polarization functions (TZ2P) as supplied with ADF and frozen-core approximations were not made.

Chemical-shielding tensors were calculated for the ^{31}P nuclei in the optimized structures by the GIAO method using the ADF

(24) Williams, T.; Kelley, C. *Gnuplot*, version 3.8j, 2002.

(25) Sheldrick, G. M. *SADABS*; Bruker AXS Inc.: Madison, WI, 2005.
(26) Sheldrick, G. M. *Acta Crystallogr., Sect. A* **1990**, *A46*, 467−473.
(27) Sheldrick, G. M. *SHELXL-97*; University of Göttingen: Göttingen, Germany, 1997.
(28) This material is available free of charge at http://www.ccdc.cam.ac.uk/data_request/cif, by emailing data_request@ccdc.ca.ac.uk, or by contacting the Cambridge Crystallographic Data Centre, 12 Union Road, Cambridge CB2 1EZ, U.K.
(29) te Velde, G.; Bickelhaupt, F. M.; Baerends, E. J.; Fonseca Guerra, C.; van Gisbergen, S. J. A.; Snijders, J. G.; Ziegler, T. *J. Comput. Chem.* **2001**, *22*, 931−967.
(30) Fonseca Guerra, C.; Snijders, J. G.; te Velde, G.; Baerends, E. J. *Theor. Chem. Acc.* **1998**, *99*, 391−403.
(31) Vosko, S. H.; Wilk, L.; Nusair, M. *Can. J. Phys.* **1980**, *58*, 1200−1211.
(32) Becke, A. D. *Phys. Rev. A* **1988**, *38*, 3098−3100.
(33) Perdew, J. P. *Phys. Rev. B* **1986**, *33*, 8822−8824.
(34) Perdew, J. P. *Phys. Rev. B* **1986**, *34*, 7406−7406.
(35) van Lenthe, E.; Baerends, E. J.; Snijders, J. G. *J. Chem. Phys.* **1993**, *99*, 4597−4610.
(36) van Lenthe, E.; Ehlers, A.; Baerends, E. *J. Chem. Phys.* **1999**, *110*, 8943−8953.
(37) van Lenthe, E.; Baerends, E. J.; Snijders, J. G. *J. Chem. Phys.* **1994**, *101*, 9783−9792.

package.[38−41] The functionals, basis sets, and relativistic approximations used were the same as those described above. The isotropic value of the absolute chemical shielding was converted to a chemical shift downfield of 85% phosphoric acid using PH_3 as a computational reference; its computed absolute shielding value was associated with a chemical shift equal to its experimental value in the gas phase.[42]

Results and Discussion

As shown in Scheme 1, our entry into diphosphaazide chemistry is provided by the sodium salt of a terminal niobium phosphide anion, $[PNb(N[Np]Ar)_3]^-$, or its $W(CO)_5$-capped derivative. While the terminal phosphide has been structurally characterized,[43] we have not previously reported on the structure of $[Na][(CO)_5WPNb(N[Np]Ar)_3]$. Red crystals of $[(Et_2O)_3Na][(CO)_5WPNb(N[Np]Ar)_3]$ were grown from diethyl ether at −35 °C. The crystals belong to the space group $P2_1/c$ and contain one molecule per asymmetric unit. The core of the molecule possesses the expected geometry of a near-linear Nb−P−W linkage with a short Nb−P bond.[44−46] The Na cation resides coordinated to the axial carbonyl, with its tetrahedral coordination sphere completed by three molecules of diethyl ether. The diethyl ether molecules and two of the anilide ligands show disorder over the lattice and were refined with the help of similarity restraints.

Alternatively, treatment of $[(Et_2O)Na][(CO)_5WPNb(N[Np]Ar)_3]$ with 2 equiv of 12-crown-4 in diethyl ether yields the bis(12-crown-4)sodium salt as a red precipitate. Diffraction-quality crystals of this compound in the space group $P2_12_12_1$ were grown from a mixture of THF and diethyl ether at −35 °C. The metric parameters of the core were similar to those of the compound without the sequestering 12-crown-4 molecules. While the 12-crown-4 linkages were themselves disordered, this disorder was removed from the vicinity of the anion. The structure of the anion is shown in Figure 1, and selected metrical parameters of the two structures are listed in Table 1.

The sodium salt of $[(CO)_5WPNb(N[Np]Ar)_3]$ reacts with Mes*NPCl to generate the $W(CO)_5$-capped niobium diphosphaazide complex, $(CO)_5W(Mes*NPP)Nb(N[Np]Ar)_3$ (**1**-$W(CO)_5$), which we had previously used only in situ. We have now realized the isolation of **1**-$W(CO)_5$ and have obtained it in pure form via crystallization from diethyl ether, though in situ generation remains the preferred method of use because of its thermal instability. Red crystals of **1**-$W(CO)_5$ grown from diethyl ether at −35 °C were subjected to an X-ray diffraction experiment from which a low-resolution solution could be determined. The connectivity was as predicted, with $W(CO)_5$ coordinated to the P_α of an η^2-bound diphosphaazide ligand. Unfortunately, anisotropic refinement was problematic without the use of heavy restraints, precluding a full discussion of metrical parameters. We were, however, able to use the geometry obtained from the crystal structure as a starting point for geometry optimization and NMR calculations on a model complex, $(CO)_5W(2,6\text{-}^tBu_2C_6H_3NPP)Nb(N[Me]Ph)_3$. The optimized structure and selected metrical parameters for this computational model are presented in Figure 2. The calculated ^{31}P NMR chemical shifts of 297 ppm (P_α) and 271 ppm (P_β) are in good agreement with the observed chemical shifts of 285 and 247 ppm.

With **3** as a target, we chose to use $(C_2H_4)Pt(PPh_3)_2$, with its labile ethylene ligand, as a trap for the $W(CO)_5(P_2)$ intermediate (Scheme 3). The addition of $(C_2H_4)Pt(PPh_3)_2$ to an in situ generated solution of **1**-$W(CO)_5$ affords no direct reaction between the starting materials, as observed by NMR spectroscopy. After stirring of the mixture for 2 h, over which time **1**-$W(CO)_5$ converts to **2**, probing by ^{31}P NMR revealed the formation of a new product with multiplet resonances at

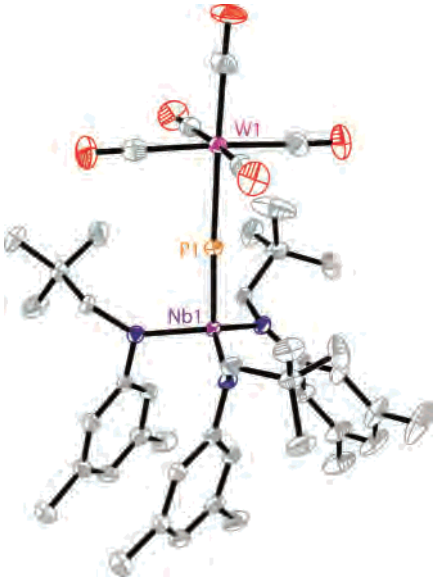

Figure 1. Crystal structure of $[(12\text{-crown-4})_2Na][(CO)_5WPNb(N[Np]Ar)_3]$ with 50% thermal ellipsoids. The H atoms and cation have been omitted for clarity.

Table 1. Selected Interatomic Distances (Å) and Angles (deg) for $[(Et_2O)_3Na][(CO)_5WPNb(N[Np]Ar)_3]$ (**A**) and $[(12\text{-crown-4})_2Na][(CO)_5WPNb(N[Np]Ar)_3]$ (**B**)

	A	B
Nb1−P1	2.2035(10)	2.2005(8)
W1−P1	2.5324(9)	2.5394(8)
Nb1−P1−W1	169.37(6)	170.79(4)
$Nb1-N_{avg}$	2.040	2.059
$W-C_{eq}$	1.945(4)	1.974(4)
$W-C_{ax}$	2.031	2.034

(38) Schreckenbach, G.; Ziegler, T. *J. Phys. Chem.* **1995**, *99*, 606−611.
(39) Schreckenbach, G.; Ziegler, T. *Int. J. Quantum Chem.* **1997**, *61*, 899−918.
(40) Wolff, S. K.; Ziegler, T. *J. Chem. Phys.* **1998**, *109*, 895−905.
(41) Wolff, S. K.; Ziegler, T.; van Lenthe, E.; Baerends, E. J. *J. Chem. Phys.* **1999**, *110*, 7689−7698.
(42) Calculated absolute chemical shieldings were converted to chemical shifts using the formula $\delta(S,calc) = \sigma(PH_3,calc) - \sigma(S,calc) + \delta(PH_3,exp)$, where $\sigma(PH_3,calc) = 577.53$ ppm and $\delta(PH_3,exp) = -266.1$ ppm. van Wüllen, C. *Phys. Chem. Chem. Phys.* **2000**, *2*, 2137−2144.
(43) Figueroa, J. S.; Cummins, C. C. *Angew. Chem., Int. Ed.* **2004**, *43*, 984−988.
(44) Scheer, M.; Kramkowski, P.; Schuster, K. *Organometallics* **1999**, *18*, 2874−2883.
(45) Johnson, B. P.; Balázs, G.; Scheer, M. *Coord. Chem. Rev.* **2006**, *250*, 1178−1195.
(46) Scheer, M.; Müller, J.; Häser, M. *Angew. Chem., Int. Ed. Engl.* **1996**, *35*, 2492−2496.
(47) Savin, A.; Nesper, R.; Wengert, S.; Fässler, T. F. *Angew. Chem., Int. Ed. Engl.* **1997**, *36*, 1808−1832.

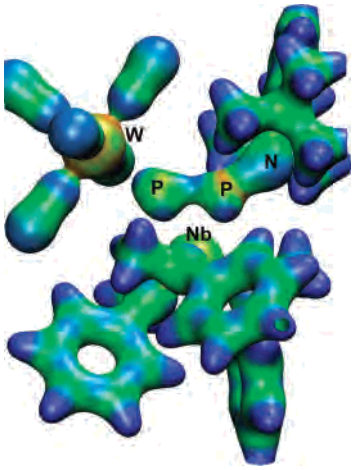

Figure 2. Optimized structure of **1m**-$W(CO)_5$ shown at an electron density isosurface value of 0.10 e/bohr^3, which is colored by the value of the electron localization function (ELF).[47] Selected interatomic distances (Å) and angles (deg): Nb−P_α 2.577; Nb−P_β 2.513; P_β−N 1.566; P_α−P_β 2.048; P_α−W 2.523; W−P_α−P_β 143.4; P_α−P_β−N 145.3; N−P_α−P_β−W −6.782.

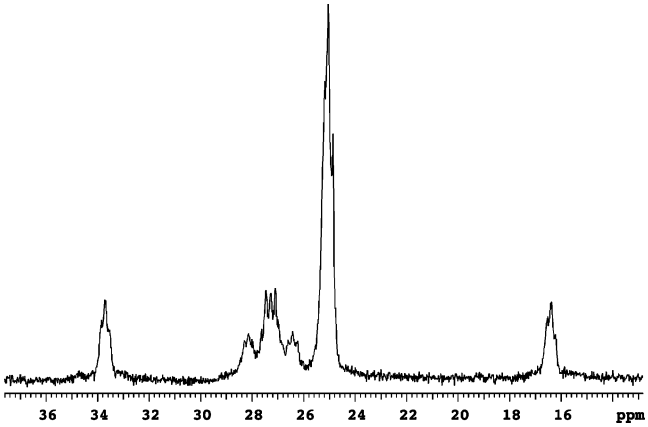

Figure 3. ^{31}P NMR spectrum of **3** in toluene at 20 °C.

Scheme 3

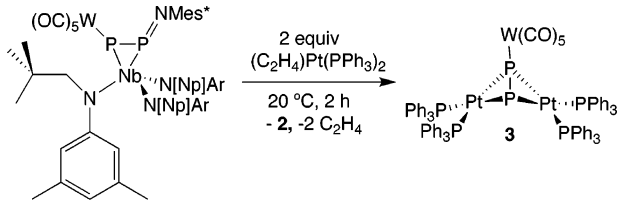

25.0 and 27.3 ppm (Figure 3); only two resonances instead of the expected four are observed. This observation can be explained by a fluxional process in which the $W(CO)_5$ unit moves back and forth between the two P atoms of the P_2 ligand at room temperature, giving chemical equivalence on the NMR time scale to all four PPh_3 units and also to the two atoms of the P_2 unit. Such behavior has been observed previously for $W_2Cp_2(CO)_4[\mu$-η^2-$P_2W(CO)_5]$.[48] We speculate on two possible mechanisms for this isomerization: (A) decoordination of the P from $W(CO)_5$ followed by inter- or intramolecular trapping or (B) slippage of $W(CO)_5$ along the π bond in the P_2 unit and onto the adjacent P. Mechanism A is less favorable because we observed this isomerization in weakly coordinating solvents (C_6D_6) that would afford little stabilization to a $W(CO)_5$ intermediate. Also, the addition of excess PPh_3 to a benzene solution of **3** does not

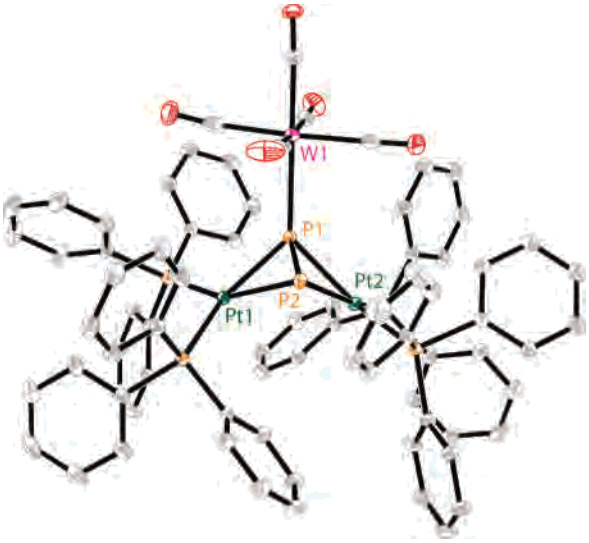

Figure 4. Crystal structure of **3** with 50% thermal ellipsoids. H atoms and toluene molecules of crystallization have been omitted for clarity. Selected interatomic distances (Å) and angles (deg): P1−P2 2.1222(10); P1−W1 2.6235(7); Pt1−P1 2.3398(7); Pt1−P2 2.4086(7); Pt2−P1 2.3897(7); Pt2−P2 2.3662(7); Pt1−P1−Pt2 91.76(2); Pt1−P2−Pt2 90.65(2); P2−P1−W1 112.67(3); Pt1−P1−P2−Pt2 105.97.

result in scavenging of the $W(CO)_5$ unit and formation of $(\mu$-$P_2)[Pt(PPh_3)_2]_2$, thus providing further evidence against mechanism A. A variable-temperature ^{31}P NMR experiment showed that at low temperatures (below 200 K) the motion of the $W(CO)_5$ unit could be frozen out, resulting in two sets of PPh_3 resonances and two signals with a large PP coupling constant (J_{PP} = 450 Hz) attributed to the μ-$(P_2)W(CO)_5$ unit (Figure S3 in the Supporting Information).

The structure of **3** was determined crystallographically using a crystal grown from toluene; 2.5 equiv of toluene cocrystallizes with **3** in the monoclinic $P2_1/n$ lattice. The structure of **3** displays the expected "butterfly" geometry, with the $W(CO)_5(P_2)$ unit bridging two Pt atoms in a μ-η^2,η^2 fashion; the remainder of each square-planar Pt coordination sphere is occupied by two triphenylphosphine ligands (Figure 4). The $W(CO)_5$ unit binds to a single P atom in the solid state, at a distance of 2.6235(7) Å. The P−P bond length of 2.1222(10) Å is significantly shorter than a P−P single bond (cf. 2.21 Å in P_4), indicating that a significant degree of multiple bonding remains despite coordination by two reducing metal centers. The average Pt−P−Pt angle across the bridge is 91°, consistent with complexation to the set of orthogonal π systems in $W(CO)_5(P_2)$. The Pt1−P1−P2−Pt2 dihedral is 105.97°.

The kinetics of the reaction generating **3** were also investigated. The decomposition of **1**-$W(CO)_5$ in the presence of $(C_2H_4)Pt(PPh_3)_2$ was monitored by ^{1}H NMR spectroscopy at 10 °C in the presence of 2.5 equiv of the platinum ethylene complex. This first-order process was found to have the same rate constant, 2×10^{-4} s^{-1}, as that observed previously for the decomposition of **1**-$W(CO)_5$ either by itself or in the presence of cyclohexadiene (Figure 5). This finding supports the hypothesis that the fragmentation releasing $W(CO)_5(P_2)$ occurs prior to any interactions between Pt (or diene) and the P_2 unit.

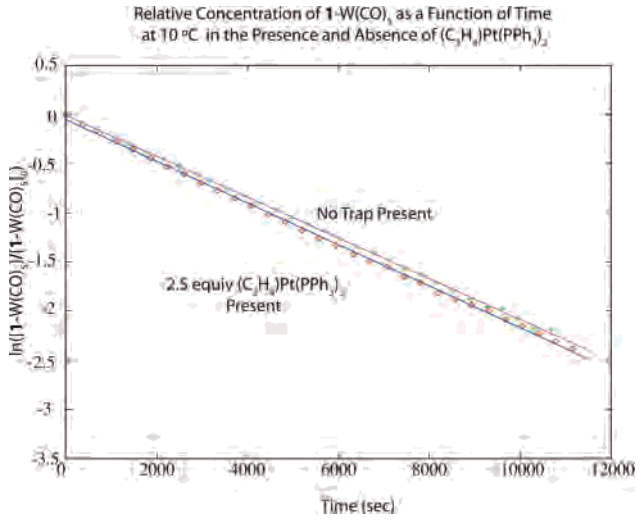

Figure 5. Decay as monitored by the normalized integral in the ^{1}H NMR spectrum of the methylene resonance of **1**-W(CO)$_5$ at 4.18 ppm. Fits to the first-order rate equation $I(t) = Ae^{-kt} + b$ give a rate constant $k = 2.1 \times 10^{-4}$ s^{-1} that is unchanged in the presence or absence of 2.5 equiv of (C_2H_4)-Pt(PPh$_3$)$_2$.

Scheme 4

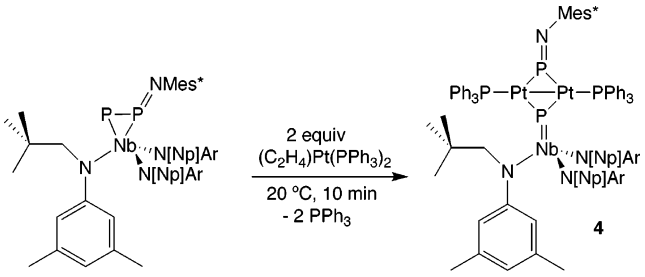

We have shown that W(CO)$_5$(P$_2$) will take up 2 equiv of either organic dienes or a platinum(0) bisphosphine, and we were interested in the possibility of generating a mixed trapping product with 1 equiv of Pt and 1 equiv of diene, namely, a coordinated cyclic (*Z*)-diphosphene. In an attempt at this, we allowed **1**-W(CO)$_5$ to fragment in the presence of (1,3-cyclohexadiene)Pt(PPh$_3$)$_2$. Unfortunately, no products incorporating the diene were observed in the NMR spectra of the products. An additional experiment involved an attempted trapping in the presence of 0.75 equiv of Pt and 10 equiv of diene, but the result was nearly exclusively bis-(diene) and Pt$_2$ trappings; additional resonances in the ^{31}P NMR spectrum of the crude reaction mixture were minor. These results can be explained by very rapid reactions of W(CO)$_5$(P$_2$) and (CO)$_5$W(P$_2$)[Pt(PPh$_3$)$_2$] with (C_2H_4)Pt(PPh$_3$)$_2$ relative to any reaction with 1,3-cyclohexadiene. The bis-(diene) trapping product is then formed only after the platinum ethylene complex is consumed.

With evidence that (C_2H_4)Pt(PPh$_3$)$_2$ is a good scavenger for W(CO)$_5$(P$_2$), we sought to trap the unstabilized free P$_2$ believed to be formed in the thermal fragmentation of **1**. However, at room temperature, treatment of **1** with 1 equiv of (C_2H_4)Pt(PPh$_3$)$_2$ affords an immediate color change from red-orange to a dark-maroon-brown. Analysis by ^{1}H and ^{31}P

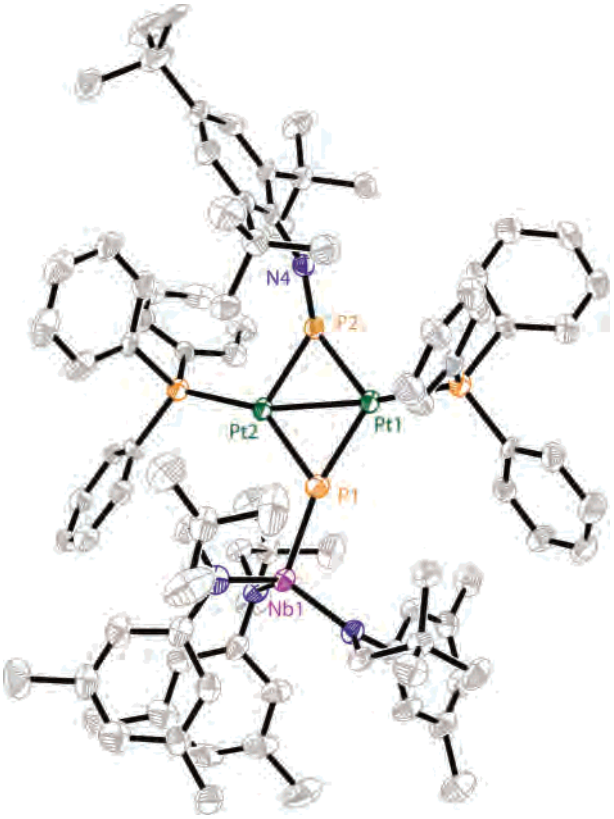

Figure 6. Crystal structure of **4** with 50% thermal ellipsoids. H atoms and molecules of solvation have been omitted for clarity. Selected interatomic distances (Å) and angles (deg): Pt1−Pt2 2.6490(13); Nb1−P1 2.2704(29); P2−N4 1.529(8); Pt1−P1 2.278(3); Pt1−P2 2.240(3); Pt2−P1 2.350(3); Pt2−P2 2.240(3); Nb1−P1−Pt2 122.7(1).

NMR spectroscopy reveals that PPh$_3$ and a new product, **4**, are generated, with $^1/_2$ equiv of **1** remaining. The addition of a second 1 equiv of (C_2H_4)Pt(PPh$_3$)$_2$ results in complete conversion to **4** (Scheme 4). On the basis of the stoichiometry of this reaction, it was inferred that 2 equiv of Pt had coordinated to the diphosphaazide ligand, which likely took on an η^1 geometry based on the large downfield chemical shift of 543 ppm observed for one of the P nuclei. To determine the exact nature of **4**, a single-crystal X-ray diffraction study was performed on a triclinic $P\bar{1}$ crystal of the 2:1 reaction product. To our surprise, the structural study revealed that the P−P bond in **1** had been cleaved, generating a bond between two three-coordinate Pt centers in a planar Pt$_2$P$_2$ diamond core (Figure 6). The two P atoms that comprise this core are both three-coordinate, distinguishing this structure from similar ones previously reported, which contain four-coordinate tetrahedral P atoms.[16,49−51] The Pt−Pt bond length of 2.6490(13) Å and the planarity at each Pt center (the sums of the angles are 358.7° around Pt1 and 359.8° around Pt2) are consistent with formulation as a Pt$^{\text{I}}$−Pt$^{\text{I}}$ bond. The Nb−P bond length of 2.2704(29) Å is

(48) Davies, J. E.; Mays, M. J.; Raithby, P. R.; Shields, G. P.; Tompkin, P. K.; Woods, A. D. *J. Chem. Soc., Dalton Trans.* **2000**, 1925−1930.

(49) Petz, W.; Kutschera, C.; Neumüller, B. *Organometallics* **2005**, *24*, 5038−5043.

(50) Gallo, V.; Latronico, M.; Mastrorilli, P.; Nobile, C. F.; Suranna, G. P.; Ciccarella, G.; Englert, U. *Eur. J. Inorg. Chem.* **2005**, 4607−4616.

(51) Taylor, N. J.; Chieh, P. C.; Carty, A. J. *J. Chem. Soc., Chem. Commun.* **1975**, 448−449.

consistent with formulation of this unit as a multiply bonded niobium phosphinidene.[43,52]

Though the direct reaction between **1** and $(C_2H_4)Pt(PPh_3)_2$ has precluded the latter's use in P_2 trapping, it has resulted in the formation of a new type of phosphinidene ligand; the chemistry of this intriguing species is being investigated. We are additionally interested in the possibility of using other coordinatively unsaturated metal complexes as traps for P_2 units.

Acknowledgment. We thank Dr. Peter Müller and Christopher C. Clough for crystallographic assistance. We acknowledge the National Science Foundation for financial support through Grant CHE-0627801 and for a predoctoral fellowship to N.A.P. We also thank Sigma-Aldrich, Inc., for a generous donation of chemicals and Thermphos International for a donation of funds for chemicals and supplies.

Supporting Information Available: Complete crystallographic data (CIF and Table S1), NMR spectral data for **3** and **4**, variable-temperature NMR spectra for **3**, electrochemical data on **4**, optimized atomic coordinates for **1m**-$W(CO)_5$, and details of mixed trapping and phosphine displacement experiments. This material is available free of charge via the Internet at http://pubs.acs.org.

IC700514U

(52) Cowley, A. H. *Acc. Chem. Res.* **1997**, *30*, 445−451.